# Embracing Uncertainty: Modeling the Standard Uncertainty in Electron Probe Microanalysis - Part I

Nicholas W. M. Ritchie
Microanalysis Group
Materials Measurement Science Division
National Institute of Standards and Technology
Gaithersburg, MD 20899-8371
nicholas.ritchie@nist.gov

August 26, 2022

**Abstract**

This is the first in a series of articles which present a new framework for computing the standard uncertainty in electron excited X-ray microanalysis measurements. This article will discuss the framework and apply it to a handful of simple but useful sub-components of the larger problem. Subsequent articles will handle more complex aspects of the measurement model. The result will be a framework in which sophisticated and practical models of the uncertainty for real-world measurements. It will include many long overlooked contributions like surface roughness and coating thickness. The result provides more than just error bars for our measurements. It also provides a framework for measurement optimization and, ultimately, the development of an expert system to guide both the novice and expert to design more effective measurement protocols.

## 1 Introduction

With the ascendancy of the silicon drift detector (SDD), energy dispersive x-ray spectrometry has attained new levels of precision and accuracy[Newbury & Ritchie, 2015, 2016a,b, 2018; Ritchie & Newbury, 2012]. Many quantitative compositional measurements which had been exclusively the purview of the wavelength-dispersive spectrometer (WDS), have become equally or better addressed with the SDD. Both detectors have strengths and weaknesses. There is no doubt that WDS is better for trace measurements and that the SDD handles softer X-rays and major and minor elements well. There has been talk about combining the strengths of both techniques as equal partners into the future electron probe microanalyzer. Not simply by collecting WDS and

energy-dispersive X-ray spectroscopy (EDS) data simultaneously (which many microprobes have done for decades), but by explicitly designing measurements around the strengths of each detector (see [Armstrong, 2014; Bullock, 2019; Camus, 2015; Moran & Wuhrer, 2016; Terborg & Richter, 2019; Thompson, 2018].) The data from both techniques would be combined, according to their strengths, into a single measurement protocol.

This is easier said than done. The electron microprobe built around WDS detectors is already considered a very complex instrument that require extensive training to operate effectively. Each measurement requires many subtle decisions for which there are few hard-and-fast rules and mostly experience and rules-of-thumb as guidance. For any given element, there may be multiple choices of characteristic X-ray lines and, for WDS, choice of monochromator. Furthermore, there are choices about sample preparation, conductive coatings, beam energy, probe current, acquisition times and other measurement parameters. A single measurement may involve tens of such decisions with complex interactions between the choices. The optimal beam energy for one element may not be the optimal beam energy for another. Depending upon the nature of the desired measurement, it may be desirable to optimize one element over another. As a result of the complexity of the measurement process, the electron microprobe operators have become like a guild where membership is earned through many years of apprenticeship with another guild-member. As we integrate the SDD into the measurement process, the choice of when to favor the SDD and when to favor the WDS makes the problem even more complex.

This is not a growth model for the electron microprobe as a measurement technique. Only a small number of problems have proven sufficiently significant that someone is willing to invest a graduate school career in becoming an electron microprobe expert. Regardless, as evidenced by the popularity of SDD on the scanning electron microscope (SEM)-platform, there is a market-based desire for measurements of composition by non-experts. Unfortunately, the marketplace has bifurcated. On one side, microprobe measurements provide reliable and robust measurements of composition for the guild-trained few and, on the other, scanning electron microscope with energy dispersive X-ray spectrometer (SEM/EDS) measurements providing sometimes accurate but sometimes inaccurate measurements to those outside the guild.

How do we, as a community, remedy this situation? How do we assist more people to make high quality measurements? How do we ensure that fewer people make poor quality measurements? The commercial EDS vendors deserve credit for making software that makes it easier to make moderate quality EDS measurements with relative ease. Standardless analysis or *remote-standards* analysis (where vendor-collected standards are used in place of locally collected standards) have made it relatively easy to make quantitative measurements albeit with unknown (and generally larger) uncertainties. When used with care on a well characterized system, remote standards can provide reasonably accurate measurements over a broad range of common measurement domains. Regardless, it remains fairly common to see in the scientific literature poor quality measurements from when the tools are misapplied. Often this happens when a

spectrum is collected from an inappropriate sample morphology but there are many other reasons.

One way to avoid this is to develop tools that help the user to design a good measurement protocol - to warn them away from pitfalls and to guide them towards best-practices. However, this is a complex problem that requires a profound level of insight into the subtleties of electron and X-ray transport, X-ray detector physics, matrix correction protocols, sample preparation and many other pieces of esoteric understanding that go into the typical electron probe micro-analysis (EPMA) measurement.

When would I benefit from adding a WDS spectrometer? Do I need a dedicated electron microprobe or is an SEM/EDS sufficient? What level of accuracy can I expect from my measurement? How well do I need to prepare my sample? What are the likely consequences of measuring my sample as is? How do I optimize my measurement for the disparate performance characteristics of the SDD and WDS? These are all difficult questions that usually require guild membership to answer.

The answers to these and many other similar questions fall under the heading of measurement optimization. Given a set of constraints, how do we design the best measurement? The constraints include such things as available instrumentation, capabilities of the instrumentation, available standards, budget (expressed in dollars or time) and sample limitations. Optimizing a measurement is dependent on being able to estimate the consequences of varying the measurement parameters. Estimating the consequences requires a profound understanding of the measurement process. In fact, optimization is closely related to the problem of placing error bars on a measurement. The optimal measurement is the one that minimizes the uncertainty within a set of constraints.

In the end, a microprobe measurement of composition is a multi-output measurement. It is not possible to measure one element without also establishing values for all the others. Measurement optimization depends upon being able to define a metric function and a set of constraints. The metric function might involve the uncertainty over all the elements simultaneously or one element alone. The constraints may include a limit on how much time the analyst is willing to expend, the availability of standards and instrumentation or the beam sensitivity of the sample. It is almost always possible to make a more precise measurement by spending more time but often time and money are limited.

Finally, this complex problem must be distilled into a solution that abstracts the complexity by only asking questions that the analyst can realistically be expected to be able to answer with the knowledge they have available. Some information is fixed and can be entered only once (instrument properties, standard material availability, etc.) while other pieces of information will need to be entered on a per-problem basis. For one, optimizing a measurement will require an estimate of the composition of the unknown. A standard-less quantitative analysis of an EDS spectrum may be a quick, effective and sufficiently accurate way to enter this information.

Clearly, this is a large and complex problem and one that can not be solved in a single article. Over the years, estimating the uncertainty associated with

microanalysis measurements has been the focus of much research[Lifshin et al., 1999; Marinenko & Leigh, 2010; Ziebold, 1967]. While much progress was made in quantifying the sources of uncertainty related to the *precision* of WDS measurements, not much progress was made being able to quantify sources of *inaccuracy* until recently[Ritchie & Newbury, 2012]. Precision is largely dependent upon instrument stability and X-ray count statistics. Accuracy is largely dependent upon matrix correction, the process of correcting the measured X-ray intensities for the physics of X-ray generation and transport. Accuracy depends upon the models and the parameters that go into the models and is complex and subjective to quantify. It is made more complex because of the circular nature of the matrix correction problem. The matrix correction depends upon the composition of the unknown which is in turn the quantity being measured. Furthermore, a complete model of the measurement uncertainty must include an understanding of the limitations of aspects of the measurement process. Take, for example, the probe current. The probe current drifts on all instruments but on some more than others. As the probe current drifts, spending more time collecting X-ray counts becomes less productive. Similarly, all probe current meters (picoammeters) have non-linearities in their response and are less than idealized measurement devices. The best standalone meters are manufacturer-specified when new to have an accuracy better than 1 % over a broad range of currents. The current meters built in to many SEMs are likely to be less well engineered and based on less high-performing digital-to-analog converters and analog electronics. As a result, they tend to be more accurate measuring similar currents than those that differ substantially. These instrument specific contributions can be modeled and included in the uncertainty.

Furthermore, there are benefits to designing measurements in which the uncertainties in certain parameters fortuitously cancel. This happens routinely when a standard similar to the unknown is selected. But there are other ways that we can work with correlations to minimize the uncertainty.

There is an unfortunate collision of language between microanalysis and statistics with respect to the word *standard*. In statistics, the phrase *standard uncertainty* can be read as the "estimated standard deviation". In microanalysis, a "standard" is a material against which we compare our unknown material. Hopefully, the use of the word standard will not be ambiguous. In this document, the modifier *standard* is often dropped and the *standard uncertainty* is simply referred to as the uncertainty.

## 1.1 Strategy

The strategy we will take to address this complex, almost overwhelming problem, is to divide it into many simpler sub-problems. The sub-problems can be pulled together in various different combinations to define the measurement model. To ensure understanding, we will provide sufficient background material to allow a typical microanalyst to follow the gist of the solution. While the solution does involve linear algebra (vectors and matrices) and basic differential calculus, the linear algebra is not that sophisticated and the differential calculus

is mostly at the introductory level.

## 1.2 Uncertainty

The ISO Guide to the Expression of Uncertainty in Measurement[JCGM (Joint Committee for Guides in Metrology), 2008] (JCGM:100) maintained by the Joint Committee for Guides in Metrology (JCGM) defines *uncertainty* as "a parameter associated with the result of a measurement, that characterizes the dispersion of the values that could reasonably be attributed to the measurand." The source of the dispersion can either be attributed to statistical fluctuations (*Type A*) or other causes (*Type B*). Type A uncertainty can be characterized by a distribution function that is selected to match an *observed frequency distribution.* Type B uncertainty is based on an *assumed probability distribution* that expresses the measurer's beliefs about measured values likely relationship with the true value.

The magnitude of both types of uncertainty is often quantified by the *estimated variance*, $u^2$. For Type A sources, the estimated variance can be calculated from an ensemble of repeat observations. For Type B sources, an estimate of the variance is constructed from the best-available information. The *standard deviation* is the positive root of the estimated variance, $\sigma = |\sqrt{u^2}|$. In the simple case, the measurand is measured directly and the uncertainty can be estimated from the measurement process. However, in many situations, the measurand is determined indirectly and is the result of a combination of $N$ other quantities some of which may be directly measured values and some of which may be model parameters. If the measurand is $Y$ and the other quantities (measurements and parameters) are $\mathbf{X} = \{X_1, X_2, \ldots, X_N\}$, the measurand can be be related to the other quantities through a *measurement model*,

$$Y = f(\mathbf{X}) = f(X_1, X_2, \ldots, X_N). \tag{1}$$

Here we are adopting the same convention as JCGM:100. The "true value" of an input variable is labeled in capital letters $\mathbf{X} = (X_1, X_2, \ldots, X_N)^\mathsf{T}$. An estimate of $\mathbf{X}$ is labeled in lower case $\mathbf{x} = (x_1, x_2, \ldots, )^\mathsf{T}$. The "true value" of the output variable is $\mathbf{Y}$ and an estimate of this dependant variable is $\mathbf{y}$. The model equations are based on the "true value" $\mathbf{Y} = \mathbf{f}(\mathbf{X})$ but all we have access to is the estimated input $\mathbf{y} = \mathbf{f}(\mathbf{x})$. The "true value" is unattainable but determining an accurate estimate of it is the aspiration of our measurement. Although the models presume knowledge of the true value, all we have access to is an estimate - the measured value - so that is what we work with. Furthermore, we will label scalars in italics (e.g., $x_i$ or $y_i$), vectors in bold (e.g., $\mathbf{X}$ or $\mathbf{x}$) and matrices in "blackboard bold" letters (e.g., $\mathbb{J}$ or $\mathbb{U}$)

Each of the $x_i$ in $\mathbf{x}$ can have associated uncertainties which will contribute to the uncertainty in $\mathbf{y}$. JCGM:100 discusses strategies for determining $u_y^2$ based on $f(\mathbf{x})$ and the uncertainties associated with the $x_i$. The primary strategy is based on a Taylor series expansion of the function about $\mathbf{x}$. This they call the *law of propagation of uncertainty.* An alternative strategy is based on a

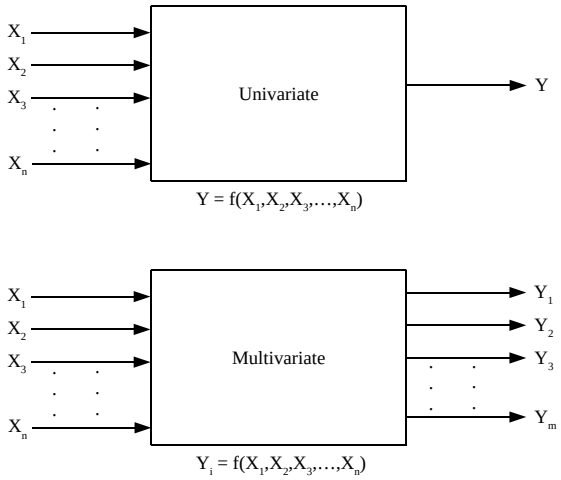


FIGURE 1: *A visualization of the difference between a* univariate measurement model *and a* multivariate measurement model.

Monte Carlo technique in which $f(\mathbf{x})$ is evaluated for many different values of $\mathbf{x}$ which are selected from the assumed probability distributions functions for the parameters. The Monte Carlo technique is discussed in detail in ISO Evaluation of Measurement Data Supplement 1 to the "Guide to the Expression of Uncertainty in Measurement" Propagation of Distributions Using a Monte Carlo Method[JCGM (Joint Committee for Guides in Metrology), 2008] (JCGM:101). For either strategy, the $x_i$ may be statistically independent or there may be correlations between two or more. The techniques in JCGM:100 and Evaluation of Measurement Data Supplement 2 to the "Guide to the Expression of Uncertainty in Measurement" Extension to Any Number of Output Quantities[JCGM (Joint Committee for Guides in Metrology), 2011] (JCGM:102) can handle any combination of dependent and independent parameters.

Both JCGM:100 and JCGM:101 focus on *univariate measurement models* - those in which there is a single measurand, $y$. However, many types of measurements involve multiple related measurands. These are called *multivariate measurement models* and require an approach that goes beyond the standard law of propagation of uncertainty as presented in JCGM:100. Figure 1 shows this distinction graphically. Even when the $X_i$ are independent, the measurement model can introduce correlations between the $Y_i$ which are not handled correctly by treating the multivariate measurement model as a set of independent univariate measurement models. The multivariate measurement model case is discussed in JCGM:102. The strategies for handling the propagation of uncertainty in multivariate measurement models are extensions of the strategies used for univariate measurement models. The law of the propagation of

uncertainties in JCGM:100 is replaced with a multivariate Taylor expansion in JCGM:102 which can be elegantly expressed using vectors and matrices. The Monte Carlo methods in JCGM:101 are easily extended to handle multivariate models.

## 1.3 The Propagation of Uncertainty

### 1.3.1 Univariate Measurement Models

JCGM:100 makes the following suggestion for calculating uncertainty in a univariate measurement process. If $Y(X_1, X_2, \dots)$ is a function of the *independent* variables (input parameters) $X_1$, $X_2, \dots$ then the uncertainty in $y$ (result estimate) can be estimated based on the first-order terms in the Taylor series expansion as

$$u_c(y(x_1, x_2, \dots)) = \left( \sum_{i=1,n} \left( \frac{\partial Y}{\partial X_i} \right)^2 u(x_i)^2 \right)^{1/2} \Bigg|_{\mathbf{X}=\mathbf{x}} . \tag{2}$$

However, if the input parameters $x_1, x_2, \dots$ are *dependent* then the combined standard uncertainty ($u_c$) of $y$ is

$$u_c(y(x_1, x_2, \dots)) = \left( \sum_{i=1,n} \left( \frac{\partial Y}{\partial X_i} \right)^2 u(x_i)^2 + 2 \sum_{\substack{i=1,n \\ k=i+1,n}} \frac{\partial Y}{\partial X_i} \frac{\partial Y}{\partial X_k} u(x_i, x_k) \right)^{1/2} \Bigg|_{\mathbf{X}=\mathbf{x}} \tag{3}$$

where $u(x_i, x_k)$ is the covariance between $x_i$ and $x_k$. $u(x_i, x_k) = u(x_i)u(x_k)\rho_{i,k}$ where $\rho_{i,k} \in [-1, 1]$ is the correlation coefficient. Note that $\rho_{i,i} = 1$ and $\rho_{i,j} = \rho_{j,i}$. The correlation coefficient can be thought of as a measure of the amount of information about $x_k$ that we can garner from a measurement of $x_i$ (or vice-versa). When the absolute value of the correlation coefficient is close to unity, then the result of one measurement tells us a lot about a measurement of the other. When the correlation coefficient is close to zero, a measurement of one tells us very little about the other (almost independent).

From these Equations 2 and 3 come the standard undergraduate formalism for propagation of uncertainty. For example, if $y = f(x_1, x_2) = \frac{x_1}{x_2}$ and $x_1$ and $x_2$ are uncorrelated (independent) then $\frac{\partial y}{\partial x_1} = \frac{1}{x_2}$ and $\frac{\partial y}{\partial x_2} = \frac{-x_1}{x_2^2}$ and

$$u_c \left( \frac{x_1}{x_2} \right)^2 = \left( \frac{1}{x_2} \right)^2 u(x_1)^2 + \left( \frac{-x_1}{x_2^2} \right)^2 u(x_2)^2 \tag{4}$$

or if $x_1$ and $x_2$ are correlated (dependent)

$$u_c \left( \frac{x_1}{x_2} \right)^2 = \left( \frac{1}{x_2} \right)^2 u(x_1)^2 + \left( \frac{-x_1}{x_2^2} \right)^2 u(x_2)^2 + 2 \left( \frac{1}{x_2} \right) \left( \frac{-x_1}{x_2^2} \right) u(x_1, x_2). \tag{5}$$

The complexity of expressions like Equation 5 has given uncertainty propagation the well-earned reputation for being unwieldy even for relatively simple measurement models.

### 1.3.2 Multivariate Measurement Models

The multivariate strategy presented in JCGM:102 is an linear algebra extension of the univariate strategy presented in JCGM:100. In JCGM:102, an explicit measurement model is expressed as a vector valued function of vector arguments, $\mathbf{Y} = \mathbf{f}(\mathbf{X})$ where $\mathbf{Y} = \{Y_1, Y_2, \ldots, Y_M\}$. The vector valued extensions of the partial derivatives is the Jacobian matrix, a $M \times N$ dimensional matrix with elements consisting of the partial derivatives $\frac{\partial Y_i}{\partial X_j}$ where $i \in [1, M]$ and $j \in [1, N]$.

$$\mathbb{J}(\mathbf{Y}) = \begin{bmatrix} \frac{\partial Y_1}{\partial X_1} & \frac{\partial Y_1}{\partial X_2} & \cdots & \frac{\partial Y_1}{\partial X_N} \\ \frac{\partial Y_2}{\partial X_1} & \frac{\partial Y_2}{\partial X_2} & \cdots & \frac{\partial Y_2}{\partial X_N} \\ \cdots & \cdots & \cdots & \cdots \\ \frac{\partial Y_M}{\partial X_1} & \frac{\partial Y_M}{\partial X_2} & \cdots & \frac{\partial Y_M}{\partial X_N} \end{bmatrix} \tag{6}$$

The uncertainties associated with the input parameters $x_i$ are expressed in an uncertainty matrix, $\mathbb{U}(\mathbf{x})$.

$$\mathbb{U}(\mathbf{x}) = \begin{bmatrix} u_1^2 & u_{1,2} & u_{1,3} & \ldots & u_{1,N} \\ u_{1,2} & u_2^2 & u_{2,3} & \ldots & u_{2,N} \\ u_{1,3} & u_{2,3} & u_3^2 & \ldots & u_{3,N} \\ \ldots & \ldots & \ldots & \ldots & \ldots \\ u_{1,N} & u_{2,N} & u_{3,N} & \ldots & u_N^2 \end{bmatrix} \tag{7}$$

where $u_i^2$ is the variance associated with $x_i$ and $u_{i,j}$ is the covariance associated with $x_i$ and $x_j$ and $u_{i,j} = u_{j,i}$. The law of propagation of uncertainties for an explicit multivariate measurement model as expressed in terms of these matrices is

$$\mathbb{U}(\mathbf{y}) = \mathbb{J}(\mathbf{Y})|_{\mathbf{X}=\mathbf{x}} \cdot \mathbb{U}(\mathbf{x}) \cdot \mathbb{J}(\mathbf{Y})^{\mathsf{T}}\Big|_{\mathbf{X}=\mathbf{x}} \tag{8}$$

It is easy to confirm that this matrix expression is equivalent for $M = 1$ to the univariate law of propagation of uncertainties (Equation 3).

The conciseness of Equation 8 is both elegant and utilitarian. It is relatively easy to implement by computer compared to the univariate equivalent in Equation 3. The bookkeeping is simplified by the matrix notation. More importantly however, Equation 8 is much easier to extend to multi-step measurement models.

Consider a composite measurement model in which $\mathbf{y}$ is broken into a series of steps. In the first step the input $\mathbf{X}$ is transformed into $\mathbf{h}(\mathbf{X})$ and then in the second step $\mathbf{h}(\mathbf{X})$ is the input to a second function, $\mathbf{f}(\mathbf{X}) = \mathbf{g}(\mathbf{h}(\mathbf{X}))$. Equation 8 can be applied directly to $\mathbf{f}(\mathbf{X})$. Alternatively, Equation 8 can be applied to

$\mathbf{h}(\mathbf{X})$ first and then to $\mathbf{g}(\mathbf{Z})$ where $\mathbf{Z} = \mathbf{h}(\mathbf{X})$.

$$\begin{aligned}\mathbb{U}(\mathbf{g}(\mathbf{h}(\mathbf{X}))) &= \mathbb{J}(\mathbf{f}(\mathbf{X})) \cdot \mathbb{U}(\mathbf{X}) \cdot \mathbb{J}(\mathbf{f}(\mathbf{X}))^{\mathsf{T}} \\ &= \mathbb{J}(\mathbf{g}(\mathbf{Z})) \cdot \left(\mathbb{J}(\mathbf{h}(\mathbf{X})) \cdot \mathbb{U}(\mathbf{X}) \cdot \mathbb{J}(\mathbf{h}(\mathbf{X}))^{\mathsf{T}}\right) \cdot \mathbb{J}(\mathbf{g}(\mathbf{Z}))^{\mathsf{T}}\Big|_{\mathbf{Z}=\mathbf{h}(\mathbf{X})} \\ &= \mathbb{J}(\mathbf{g}(\mathbf{Z}))|_{\mathbf{Z}=\mathbf{h}(\mathbf{X})} \cdot \mathbb{J}(\mathbf{h}(\mathbf{X})) \cdot \mathbb{U}(\mathbf{X}) \cdot \left(\mathbb{J}(\mathbf{g}(\mathbf{Z}))|_{\mathbf{Z}=\mathbf{h}(\mathbf{X})} \cdot \mathbb{J}(\mathbf{h}(\mathbf{X}))\right)^{\mathsf{T}}\end{aligned} \tag{9}$$

where $\mathbb{J}(\mathbf{h}(\mathbf{X})) \cdot \mathbb{U}(\mathbf{X}) \cdot \mathbb{J}(\mathbf{h}(\mathbf{X}))^{\mathsf{T}} = \mathbb{U}(\mathbf{h}(\mathbf{X}))$. For complex measurement models, it often easier to evaluate the Jacobians of $\mathbf{h}(\mathbf{X})$ and $\mathbf{g}(\mathbf{Z})$ than the Jacobian of $\mathbf{g}(\mathbf{h}(\mathbf{X}))$.

This step-wise approach is not an approximation as can be demonstrated through the chain rule of differential calculus. The chain-rule for a function of a single variable states that if $f(x) = g(h(x))$ then

$$\frac{\partial f(x)}{\partial x} = \frac{\partial g}{\partial z}\bigg|_{Z=h(x)} \frac{\partial h}{\partial x} \tag{10}$$

For a vector function of a vector argument, the chain rule can be expressed in terms of the Jacobians. If $\mathbf{f}(\mathbf{X}) = \mathbf{g}(\mathbf{h}(\mathbf{X}))$ then the multivariate equivalent of the chain rule is

$$\mathbb{J}(\mathbf{f}(\mathbf{X})) = \mathbb{J}(\mathbf{g}(\mathbf{Z}))|_{\mathbf{Z}=\mathbf{h}(\mathbf{X})} \mathbb{J}(\mathbf{h}(\mathbf{X})). \tag{11}$$

The chain rule can be applied recursively as necessary to construct a final Jacobian that is the product of an arbitrary number of chained Jacobians. The final Jacobian will have rows associated with the output variables and columns associated with the input variables. The intermediate Jacobians will have varying numbers of rows and columns as the inputs are transformed into intermediate values and intermediate values are transformed into yet other intermediate values until the final step transforms intermediate values into the output values.

The chain rule allows us to decompose a complex multi-variate measurement model into a series of simpler steps without any additional approximations. The final Jacobian makes it possible to track the uncertainty contributions from the input variables through complex measurement models to the output variables. This permits an analysis of the sensitivity of the output values to the input parameters. The Jacobian is also useful for optimization. The Jacobian can also be used to implement a gradient-descent optimization scheme to efficiently predict the optimal experimental parameters.

## 1.4 Implicit Models

Up to this point, we have considered measurement models taking the *explicit* form

$$\mathbf{Y} = \mathbf{f}(\mathbf{X}). \tag{12}$$

Many practical models fall into this class, however, matrix correction requires a more general form called an *implicit multivariate measurement model*. An implicit measurement model is one in which the relationship between the input quantity $\mathbf{X}$ and the output quantity $\mathbf{Y}$ can not be expressed in the form in Equation 12 but must be expressed in the more general form

$$\mathbf{h}(\mathbf{Y}, \mathbf{X}) = \mathbf{0} \tag{13}$$

where $\mathbf{h} = (h_1, h_2, \ldots, h_{n_y})^\mathsf{T}$. An estimate of the quantity $\mathbf{Y}$, $\mathbf{y}$, given a measurement of $\mathbf{X}$, $\mathbf{x}$, is given by the solution to

$$\mathbf{h}(\mathbf{y}, \mathbf{x}) = \mathbf{0}. \tag{14}$$

The associated covariance matrix of $y$ is an $n_y \times n_y$ matrix defined by the equation

$$\mathbb{J}_\mathbf{y} \mathbb{U}_\mathbf{y} {\mathbb{J}_\mathbf{y}}^\mathsf{T} = \mathbb{J}_\mathbf{x} \mathbb{U}_\mathbf{x} {\mathbb{J}_\mathbf{x}}^\mathsf{T} \tag{15}$$

where $\mathbb{J}_\mathbf{y}$ is the Jacobian matrix containing the partial derivatives of $\mathbf{h}$ with respect to $\mathbf{Y}$ and $\mathbb{J}_\mathbf{x}$ is the Jacobian matrix containing the partial derivatives of $\mathbf{h}$ with respect to $\mathbf{X}$. The derivatives are evaluated at $\mathbf{Y} = \mathbf{y}$ and $\mathbf{X} = \mathbf{x}$.

For example, in EPMA measurements we measure the $k$-ratio, defined as the ratio of the measured X-ray intensity on the unknown over the measured intensity on a standard under similar measurement conditions, and apply a measurement model to convert a set of $k$-ratios into measures of composition. It is not possible to write the $k$-ratio measurement model in an explicit form (see Equation 12). The $k$-ratio measurement model can however be written in the implicit form (see Equation 14) as a set of coupled equations

$$k_i - \frac{C_{u,i}}{C_{s,i}} \frac{ZAF_{u,i}(\mathbf{C}_u)}{ZAF_{s,i}(\mathbf{C}_s)} = \delta_i, \tag{16}$$

where $i$ indexes the elements in the unknown and $C_{s,i}$ is the mass fraction of the $i$-th element in the standard, $\frac{ZAF_{u,i}(\mathbf{C}_u)}{ZAF_{s,i}(\mathbf{C}_s)}$ is the matrix correction factor for unknown relative to the standard, and $\mathbf{C}_u$ is the composition of the unknown for all $i$. We wish to find the $\mathbf{C}_{unk}$ such that each of the $\delta_i$ are sufficiently close to zero. The process of solving for the $\mathbf{C}_u$ has classically been called "iteration" in the field of X-ray microanalysis but, from a mathematical perspective, it is an root-finding problem.

It is worth noting that, in practice, the termination criterion for the iteration procedure is not typically based on the difference between the computed $k$-ratio and the measured as suggested here. Instead the termination criterion has been based on the the change in the estimated $C_i$ from iteration step to iteration step. For example, see Figure 12.1 in Heinrich[Heinrich, 1981] and the source code for CalcZAF (`https://github.com/openmicroanalysis/calczaf/blob/master/zaf.bas`, commit 9ab9414, lines 2016-2022). While minimizing the change in $C_i$ is a necessary criterion for convergence and may work in practice, it

is not sufficient. The correct convergence criterion is minimizing $\delta_i$ in Equation 16. Convergence criteria based on change in $C_i$ are not equivalent. Further investigation is necessary to determine if this is a problem in practice.

Iteration converges quickly and reliably to 4 significant figures using Wegstein iteration[Reed & Mason, 1967] in 3 or 4 steps for binary unknowns[Springer, 1976] and, in the authors experience, less than 10 steps for multi-element unknowns. In the authors experience, it is necessary to normalize the mass-fraction inputs to $\frac{ZAF_{u,i}(\mathbf{C}_u)}{ZAF_{s,i}(\mathbf{C}_s)}$ (but not the other $C_{u,i}$ and $C_{s,i}$ in Equation 16) to ensure convergence. Other iteration algorithms generally converge slower[Springer, 1976] and some fail to converge in certain circumstances like soft X-rays in highly absorbing matrices[Pouchou & Pichoir, 1991].

# 2 Building the Pieces

We will start with some simple but useful examples of applying JCGM:102 to EPMA calculations. In these cases, calculating the partial derivatives for the Jacobian (see Equation 6) is relatively straightforward.

## 2.1 Expressions of Composition

Measures of composition serve as both inputs and the output of a typical X-ray microanalysis measurement. The input compositions can have associated uncertainties which, in some cases, may represent a significant source of measurement uncertainty. Historically, the uncertainty in the composition of the standards has been largely ignored. It is worth noting that no standard is perfect and even pure elements standards often have native oxide surface layers and/or trace impurities. This is particularly true for engineered or natural materials which may also have unanticipated inhomogeneities.

The output compositions may need to be transformed from one representation to another. In the following sections, the set of mass fractions is represented by $\{C_i\}$, the set of normalized mass fractions by $\{N[C_i]\}$, the set of atom fractions by $\{A_i\}$, the set of material fractions by $\{M_i\}$, and the set of material dependent atomic weights by $\{\mathscr{A}_i\}$.

### 2.1.1 Mass Fraction to Atom Fraction

The composition of a material is expressed in a handful of common representations. In microanalysis, the most basic representation is as mass-fractions as these are the natural inputs and output of the $k$-ratio correction model. However, it is often desirable to report the composition as the normalized mass fraction, the atom fraction or the oxide fraction. To convert from mass-fraction ($C_i$) to atom-fraction ($A_i$),

$$A_i = \frac{C_i/\mathscr{A}_i}{\sum_k C_k/\mathscr{A}_k}. \tag{17}$$

A)

$$\begin{bmatrix} \textit{Quantity} & \textit{Value} \\ C_{Ag} & 0.4020 \\ C_{Au} & 0.5950 \\ N[C_{Ag}] & 0.4032 \\ N[C_{Au}] & 0.5968 \\ A_{Ag} & 0.5523 \\ A_{Au} & 0.4477 \\ \textit{Total} & 0.9970 \\ \overline{Z} & 65.8990 \\ \overline{\mathscr{A}} & 160.5583 \end{bmatrix} \pm \begin{bmatrix} C_{Ag} & C_{Au} & N[C_{Ag}] & N[C_{Au}] & A_{Ag} & A_{Au} & \textit{Total} & \overline{Z} & \overline{\mathscr{A}} \\ (0.0090)^2 & – & – & – & – & – & – & – & – \\ – & (0.0120)^2 & – & – & – & – & – & – & – \\ – & – & (0.0073)^2 & -1.00 \cdot \sigma_R\sigma_C & 1.00 \cdot \sigma_R\sigma_C & -1.00 \cdot \sigma_R\sigma_C & -0.09 \cdot \sigma_R\sigma_C & -0.31 \cdot \sigma_R\sigma_C & -0.34 \cdot \sigma_R\sigma_C \\ – & – & -1.00 \cdot \sigma_R\sigma_C & (0.0073)^2 & -1.00 \cdot \sigma_R\sigma_C & 1.00 \cdot \sigma_R\sigma_C & 0.09 \cdot \sigma_R\sigma_C & 0.31 \cdot \sigma_R\sigma_C & 0.34 \cdot \sigma_R\sigma_C \\ – & – & 1.00 \cdot \sigma_R\sigma_C & -1.00 \cdot \sigma_R\sigma_C & (0.0075)^2 & -1.00 \cdot \sigma_R\sigma_C & -0.09 \cdot \sigma_R\sigma_C & -0.31 \cdot \sigma_R\sigma_C & -0.34 \cdot \sigma_R\sigma_C \\ – & – & -1.00 \cdot \sigma_R\sigma_C & 1.00 \cdot \sigma_R\sigma_C & -1.00 \cdot \sigma_R\sigma_C & (0.0075)^2 & 0.09 \cdot \sigma_R\sigma_C & 0.31 \cdot \sigma_R\sigma_C & 0.34 \cdot \sigma_R\sigma_C \\ – & – & -0.09 \cdot \sigma_R\sigma_C & 0.09 \cdot \sigma_R\sigma_C & -0.09 \cdot \sigma_R\sigma_C & 0.09 \cdot \sigma_R\sigma_C & (0.0150)^2 & 0.98 \cdot \sigma_R\sigma_C & 0.97 \cdot \sigma_R\sigma_C \\ – & – & -0.31 \cdot \sigma_R\sigma_C & 0.31 \cdot \sigma_R\sigma_C & -0.31 \cdot \sigma_R\sigma_C & 0.31 \cdot \sigma_R\sigma_C & 0.98 \cdot \sigma_R\sigma_C & (1.0381)^2 & 1.00 \cdot \sigma_R\sigma_C \\ – & – & -0.34 \cdot \sigma_R\sigma_C & 0.34 \cdot \sigma_R\sigma_C & -0.34 \cdot \sigma_R\sigma_C & 0.34 \cdot \sigma_R\sigma_C & 0.97 \cdot \sigma_R\sigma_C & 1.00 \cdot \sigma_R\sigma_C & (2.5552)^2 \end{bmatrix}$$

B)

| *Element* | $Z$ | $\mathscr{A}$ | *Mass Fraction* | *Normalized Mass* | *Atom Fraction* |
|---|---|---|---|---|---|
| Silver | 47 | $107.87 \pm 0.00$ | $0.4020 \pm 0.0090$ | $0.4032 \pm 0.0073$ | $0.5523 \pm 0.0075$ |
| Gold | 79 | $196.97 \pm 0.00$ | $0.5950 \pm 0.0120$ | $0.5968 \pm 0.0073$ | $0.4477 \pm 0.0075$ |
| *Mean/Total* | $65.90 \pm 1.04$ | $160.56 \pm 2.56$ | $0.9970 \pm 0.0150$ | 1.0000 (exact) | 1.0000 (exact) |

TABLE 1: *Two different representations of the composition of a Gold/Silver alloy expressed as mass fraction ($C_i$), normalized mass fraction ($N[C_i]$), atom fraction ($A_i$), analytical total (Total), mean atomic number ($\overline{Z}$) and mean atomic weight ($\overline{\mathscr{A}}$). A) Shows the full details of the uncertainty matrix. The values for each quantity are listed in the left-hand matrix and the variances and covariances in the right-hand matrix. To facilitate interpretation, the diagonal matrix elements (the variances) are formatted as the square of the $\sigma$, the uncertainty, and the off-diagonal elements are shown as the correlation coefficient times $\sigma_R$ and $\sigma_C$, the uncertainties associated with the covariance's row and column. B) shows a subset of this information, namely the values and the uncertainties. B) is the appropriate representation when reporting final results as these uncertainties represent the best estimate of the observed uncertainties. However, A) is the optimal representation if these values are going to be used in subsequent calculations.*

$$\frac{\partial A_i}{\partial C_j} = \begin{cases} \frac{A_i(1-A_i)}{C_i} & \text{if } i = j, \\ \frac{-A_i A_j}{C_j} & \text{if } i \neq j. \end{cases}$$

$$\frac{\partial A_i}{\partial \mathscr{A}_j} = \begin{cases} \frac{A_i(A_i-1)}{\mathscr{A}_i} & \text{if } i = j, \\ \frac{A_i A_j}{\mathscr{A}_j} & \text{if } i \neq j. \end{cases}$$

The Jacobian is an $N \times 2N$ matrix where $N$ is the number of elements. The input uncertainty matrix is $2N \times 2N$ for each of the $A_i$ and $\mathscr{A}_i$ and the output uncertainty matrix is $N \times N$. The resulting atom fractions are normalized to 100 % regardless of the normalization of the mass fractions.

### 2.1.2 Mass Fraction to Normalized Mass Fraction

Normalization is a common practice in compositional measurements and other fields in which the result is expressed as a fraction or percent of the whole. In

EPMA, each element is measured independently so the *analytical total*, defined as the sum of mass fractions over all elements, does not necessarily equal unity. However, the deviation of the analytical total from unity is useful for appraising the reliability of a measurement. While a measurement that totals close to unity is not guaranteed to be accurate, deviation of more than 1 mass % to 2 mass % from unity is a clue that there is likely to be a problem.

Normalization of a set of quantities, $\{x_i\}$ is defined

$$N[x_i] = \frac{x_i}{\sum_k x_k} \tag{18}$$

$$\frac{\partial N[x_i]}{\partial x_j} = \begin{cases} \frac{N[x_i](1-N[x_i])}{x_i} & \text{for } i = j, \\ -\frac{N[x_i]^2}{x_i} & \text{otherwise.} \end{cases}$$

Normalizing mass fraction results improves the calculated error budget because the number of degrees-of-freedom is reduced by one. However, normalization does not always improve the accuracy. In part, it depends on whether the deviation from unity is statistical or systematic. If an element is omitted from the analysis, normalizing is likely only to mis-attribute this error to the measured elements. However, even when the deviation is statistical, individual uncertainty components can increase through normalization. Typically, the uncertainty associated with major element constituents improve and those associated with minor and trace quantities deteriorate.

### 2.1.3 Element-by-Difference

While typically the uncertainty calculations for compositional measures are relatively simple, one must be careful. For example, it is quite common for a material to be defined in terms of quantities of certain minor or alloying elements with the remainder being made up of the majority element. For example, stainless steel 304 (SS-304) is defined as 18 % to 20 % Cr and 8.0 % to 10.5 % Ni (with trace quantities of C which we will ignore for this example) and the remainder being Fe. You might be tempted to define SS-304 in terms of three independent uncertainties as [ (Cr, $0.19 \pm 0.01$), (Ni, $0.0925 \pm 0.0125$) and (Fe, $0.7175 \pm 0.0160$) by mass] where $0.01^2 + 0.0125^2 = 0.0160^2$ as shown in Table 2. However, this is not correct because there is the explicit constraint that the sum of the elements must be unity that is not consistent with the assumption of independence. The *element-by-difference* scenario happens when defining standards and when it is used to estimate hard-to-measure elements during the iteration process.

The Jacobian consists of $N$ output rows and $N - 1$ input columns.

$$C_N^* = 1 - \sum_{j=1}^{N-1} C_j \tag{19}$$

A)

| *Element* | *Z* | *A* | *Mass Fraction* | *Normalized Mass* | *Atom Fraction* |
|---|---|---|---|---|---|
| Chromium | 24 | $52.00 \pm 0.00$ | $0.1900 \pm 0.0100$ | $0.1900 \pm 0.0100$ | $0.2021 \pm 0.0105$ |
| Iron | 26 | $55.84 \pm 0.00$ | $0.7175 \pm 0.0160$ | $0.7175 \pm 0.0160$ | $0.7107 \pm 0.0159$ |
| Nickel | 28 | $58.69 \pm 0.00$ | $0.0925 \pm 0.0125$ | $0.0925 \pm 0.0125$ | $0.0872 \pm 0.0118$ |
| *Mean/Total* | $25.81 \pm 0.03$ | $55.38 \pm 0.05$ | 1.0000 (exact) | 1.0000 (exact) | 1.0000 (exact) |

B)

| *Element* | *Z* | *A* | *Mass Fraction* | *Normalized Mass* | *Atom Fraction* |
|---|---|---|---|---|---|
| Chromium | 24 | $52.00 \pm 0.00$ | $0.1900 \pm 0.0100$ | $0.1900 \pm 0.0090$ | $0.2021 \pm 0.0094$ |
| Iron | 26 | $55.84 \pm 0.00$ | $0.7175 \pm 0.0160$ | $0.7175 \pm 0.0123$ | $0.7107 \pm 0.0122$ |
| Nickel | 28 | $58.69 \pm 0.00$ | $0.0925 \pm 0.0125$ | $0.0925 \pm 0.0115$ | $0.0872 \pm 0.0109$ |
| *Mean/Total* | $25.81 \pm 0.59$ | $55.38 \pm 1.27$ | $1.0000 \pm 0.0226$ | 1.0000 (exact) | 1.0000 (exact) |

TABLE 2: *The composition of SS304 defined using A) Fe by difference and B) the assumption of independence. The differences are pronounced in the* Mean/-Total *row in which the uncertainties associated are clearly different. When the element-by-difference assumption is made, the uncertainty in the mass fraction total is zero in A) but is 0.0226 in B). Normalizing the composition doesn't change the uncertainties in A) because a sum of unity is built in but normalization makes a spurious difference in B). Furthermore, the individual normalized uncertainties are different from A) to B) as is also the case in the atom fraction column.*

$$\frac{\partial C_N^*}{\partial C_j} = -1$$

The difference between the naive model of independence and this more careful model is demonstrated in the example in Table 2.

### 2.1.4 Element-by-Stoichiometry

Element-by-stoichiometry is implemented by assigning to each element, $z_j$, an integer valence, $v_j$, a measure of its affinity to combine with other elements. Molecules tend to form in elemental ratios in which the sum of the valences is balanced (equals zero). The most common element which is quantified using valence is oxygen which has a valence, $v_O = -2$. Other elements which may combine with oxygen have a positive valence, like $v_{Al} = 3$, $v_{Si} = 4$. Two atoms of aluminum combine with three atoms of oxygen ($Al_2O_3$) to give a net valence of $2v_{Al} + 3v_O = 0$ and one atom of silicon combines the two atoms of oxygen ($SiO_2$) to give a net valence of $V_{Si} + 2V_O = 0$. If $N$ is the index of the element-by-stoichiometry calculated from the $N-1$ other elements,

$$C_N^* = \frac{\mathscr{A}_N}{-v_N} \sum_{j=1}^{N-1} \left( \frac{v_j}{\mathscr{A}_j} \right) C_j \tag{20}$$

$$\frac{\partial C_N^*}{\partial C_j} = \frac{\mathscr{A}_N}{-v_N} \frac{v_j}{\mathscr{A}_j}$$

$$\frac{\partial C_N^*}{\partial \mathscr{A}_j} = \begin{cases} \frac{\mathscr{A}_N}{-v_N}\left(\frac{-v_j}{\mathscr{A}_j^2}\right) C_j & \text{for } j \neq N \\ \frac{C_N^*}{\mathscr{A}_N} & \text{for } j = N \end{cases}$$

This model does not address the problem of multi-valent cations. However, it would not be difficult to create a model in which the material is a fractional mixture of an element's cations with different valences with an uncertainty in the fractional proportions.

### 2.1.5 Atom Proportion to Normalized Mass Fraction

Converting from atom proportion to mass fraction is routine when dealing with stoichiometric compounds or materials initially expressed in terms of the relative number of atoms (expressed either as a fraction or as stoichiometry). The results is necessarily normalized to unity. In theory, atom proportions can be without error as we could, at least in theory, count the individual atoms in a material with absolute precision. The resulting mass fraction will always have the additional uncertainty contributed by the elemental atomic weights.

$$N[C_i] = \frac{A_i \mathscr{A}_i}{\sum_k A_k \mathscr{A}_k}. \tag{21}$$

$$\frac{\partial N[C_i]}{\partial A_j} = \begin{cases} \frac{N[C_i](1-N[C_i])}{A_i} & \text{for } i = j, \\ \frac{-N[C_i]N[C_j]}{A_j} & \text{for } i \neq j. \end{cases}$$

$$\frac{\partial N[C_i]}{\partial \mathscr{A}_j} = \begin{cases} \frac{N[C_i](1-N[C_i])}{\mathscr{A}_i} & \text{for } i = j, \\ \frac{-N[C_i]N[C_j]}{\mathscr{A}_j} & \text{for } i \neq j. \end{cases}$$

These expressions demonstrate that even when the input uncertainty matrix is diagonal, meaning that the uncertainties for each element are uncorrelated, the output uncertainty matrix will have correlations between element $i$ and element $j$, $i \neq j$, whenever $\frac{\partial Y_i}{\partial X_j} \neq 0$.

### 2.1.6 Mixtures

Many geological material exist in pure end-member forms and also in mixtures of end-members. For example, feldspar is a tectosilicate mineral with three end-members, potassium feldspar $KAlSi_3O_8$, albite $NaAlSi_3O_8$ and anorthite $CaAl_2Si_2O_8$. It is common to find individual crystals with a range of admixtures of potassium feldspar, albite and anorthite. These minerals in which "a crystal containing a second constituent which fits into and is distributed in the lattice of the host crystal" are often called *solid solutions* though the preferred name is *mixed crystals*[McNaught & Wilkinson, 2020]. Similarly, engineered glasses are

A)

| *Material* | *Mass Fraction* | *Uncertainty* |
|---|---|---|
| MgO | 0.1933 | 0.002 |
| FeO | 0.0996 | 0.002 |
| $SiO_2$ | 0.4535 | 0.002 |
| CaO | 0.1525 | 0.002 |
| $Al_2O_3$ | 0.0927 | 0.002 |

B)

| *Element* | *Z* | *Mass Fraction* | *Norm. Mass* | *Atom Frac.* |
|---|---|---|---|---|
| Fe | 26 | $0.0774 \pm 0.0014$ | $0.0781 \pm 0.0013$ | $0.0308 \pm 0.0006$ |
| Al | 13 | $0.0491 \pm 0.0010$ | $0.0495 \pm 0.0009$ | $0.0404 \pm 0.0008$ |
| O | 8 | $0.4276 \pm 0.0006$ | $0.4312 \pm 0.0012$ | $0.5940 \pm 0.0011$ |
| Ca | 20 | $0.1090 \pm 0.0012$ | $0.1099 \pm 0.0011$ | $0.0604 \pm 0.0007$ |
| Si | 14 | $0.2120 \pm 0.0005$ | $0.2138 \pm 0.0006$ | $0.1678 \pm 0.0004$ |
| Mg | 12 | $0.1166 \pm 0.0010$ | $0.1176 \pm 0.0009$ | $0.1066 \pm 0.0008$ |
| Totals | - | $0.9916 \pm 0.0024$ | 1.000(exact) | 1.000 (exact) |

TABLE 3: *An example of calculating the elemental composition of the glass K412 as define in the NIST SRM-470 certificate in terms of a melt of the constituent oxides shown in A). Note that there is an implicit normalization operation that is not represented in the uncertainties in A). While the uncertainty in any one of the constituent materials might be 0.0020, the sum of mass fractions must be unity. B) shows the mass fraction, normalized mass fraction and atom fraction for the elemental constituents as calculated from A).*

often defined defined by the mass of the constituent oxides in the melt. Assume that we have mixture of $N$ materials of masses $M_i$ and with mass fraction of element $z$, $C_{i,z}$.

The mass fraction in the resulting mixture is

$$C_{M,z} = \sum_{i=1}^{N} M_i C_{i,z} \tag{22}$$

$$\frac{\partial C_{M,z}}{\partial M_j} = C_{j,z} \qquad \frac{\partial C_{M,z}}{\partial C_{j,z}} = M_{j,z}$$

It is possible (albeit unusual) that the isotopic abundances in each material are different so we assign a material dependent atomic weight $\mathscr{A}_{i,z}$ to each element in each material. The atomic weight of the resulting material for element $z$ is

$$\mathscr{A}_{M,z} = \frac{\sum_{i=1}^{N} M_i C_{i,z}}{\sum_{i=1}^{N} \frac{M_i C_{i,z}}{\mathscr{A}_{i,z}}} \tag{23}$$

$$\frac{\partial \mathscr{A}_{M,z}}{\partial M_j} = \frac{C_{j,z}}{\sum_{i=1}^{N} M_i C_{i,z}} \left( A_{M,z} - A_{M,z}^2 / A_{j,z} \right)$$

$$\frac{\partial \mathscr{A}_{M,z}}{\partial C_{j,z}} = \frac{M_j}{\sum_{i=1}^{N} M_i C_{i,z}} \left( A_{M,z} - A_{M,z}^2 / A_{j,z} \right)$$

$$\frac{\partial \mathscr{A}_{M,z}}{\partial A_{j,z}} = \frac{C_{M,z} A_{M,z}^2}{A_{j,z}}$$

A practical calculation might proceed in the following manner. Given a mass fraction, we might want to express the same composition in normalized mass fractions and atomic fraction forms.

Anorthoclase ($[\mathrm{K}, \mathrm{Na}](\mathrm{AlSi_3O_8})$) is an intermediate between mineral endmembers sanidine ($\mathrm{K}(\mathrm{AlSi_3O_8})$) and albite ($\mathrm{Na}(\mathrm{AlSi_3O_8})$). We might know that a particular instance of anorthoclase is $(40.0 \pm 0.1)$ mass % sanidine and $(60.0 \pm 0.1)$ mass % albite. The first step in the calculation would involve transforming sanidine which is 1/13 K, 1/13 Al, 3/13 Si and 8/13 O by atomic fraction and albite which is 1/13 Na, 1/13 Al, 3/13 Si and 8/13 O into normalized mass fractions. The second step would involve computing the mixture of 0.4 sanidine by mass and 0.6 albite by mass. The steps would be combined using Equation 11.

## 2.2 Mass Absorption Coefficients

Mass absorption coefficients (MACs) have been a long identified source of uncertainty in X-ray microanalysis. A thin foil or gas of an element will absorb X-rays through photo-ionization. The magnitude of the transmission through a thin foil or gas is described by Beer's Law. The absorption is a function of

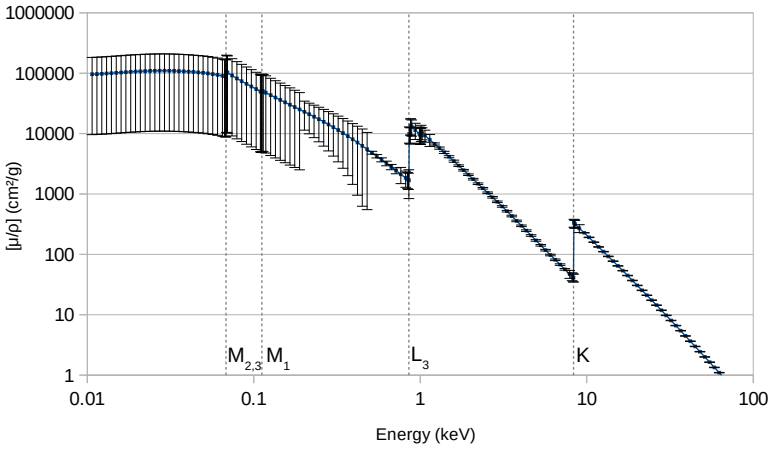


FIGURE 2: *The elemental mass absorption coefficient (MAC) for Ni according to the FFAST database (https://physics.nist.gov/cgi-bin/ffast/ffast.pl?Z=28&Formula=&gtype=4&range=S&lower=0.001&upper=1000&density= downloaded 19-Nov-2018). The overall trend is towards smaller coefficients as energy increases but there are a number of energies at which the mass absorption coefficient (MAC) increases abruptly. These energies are labeled with the associated ionization edge. The error bars represent the uncertainties computed using the rules specified by Chantler[Chantler, 2000] with the following modifications. When an energy matched more than one rule, the rule giving the largest uncertainty was selected and the maximum fractional uncertainty was limited to 90 %.*

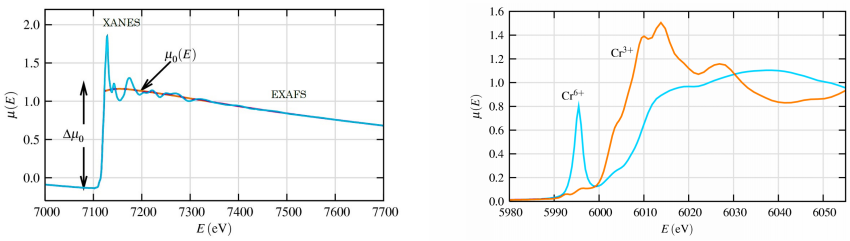


(A) *FeO* (B) *$Cr^{+3}$ and $Cr^{+6}$ oxides*

FIGURE 3: *(A) A measured XAFS spectrum from FeO showing XANES and EXAFS regions (blue) and a smoothed background function (red). (B) XANES structure for the $Cr^{+3}$ and $Cr^{+6}$ oxides. (From [Newville, 2004])*

the X-ray energy as expressed by the elemental MAC, $[\mu/\rho]_Z$ where normalizing by the density, $\rho$, eliminates the need to know this quantity. An example of an elemental MAC is shown in Figure 2. It shows some of the typical characteristics. The MAC overall decreases with increasing X-ray energy except around the photoionization absorption edge energies and at low energies.

Typically, an EDS measurement of an element involves multiple lines in a family often with similar energies. We would expect that the elemental mass absorption coefficients for lines that are of similar energies to be correlated. If the tabulated mass absorption coefficient is low for one energy, we expect the mass absorption coefficient to be low for other nearby energies. The exception to this is near absorption edges where often the magnitude of the mass absorption coefficient varies over a range of tens to hundreds of electron-volts due to near edge structure (see Figure 3). The energy of the edge can also shift, particularly if a valence electron participates is the transition. When the edge shifts, the characteristic X-rays can fall below the edge in one material and on the edge in others. This leads to a large uncertainty and a low level of correlation between X-rays very close above and below the edge. This is not really an issue for WDS measurements in which usually only one characteristic X-ray transition per element participates in the measurement. However, in EDS measurements multiple proximate lines participate in each measurement. Assuming the uncertainty in the mass absorption coefficient between lines is independent overestimates the total uncertainty.

Samples are typically not pure elements and creating an exhaustive set of material MACs is unrealistic so the material MAC is typically computed from the pure elemental MAC for an energy, $E$, using

$$[\mu/\rho](\mathbf{C}, E) = \sum_Z C_Z [\mu/\rho]_Z (E) \tag{24}$$

$$\frac{\partial [\mu/\rho](\mathbf{C}, E)}{\partial C_Z} = [\mu/\rho]_Z (E)$$

$$\frac{\partial[\mu/\rho]\left(\mathbf{C},E\right)}{\partial[\mu/\rho]_Z\left(E\right)} = C_Z$$

This expression is essentially equivalent to considering the absorption from each element as independent. The presence of the other elements has no influence. To a certain extent, this makes sense since the photo-ionization typically occurs on core shells where chemistry and solid-state effects have little influence. However, there are situations in which the other elements through chemistry or crystallography will influence the photo-ionization. We will discuss this model breakdown and some thoughts on how to handle it.

The uncertainty in the composition comes either from the uncertainty in the standard or as part of solving for the uncertainty in the unknown as we will see in section 2.4. For uncertainty in the MAC, we will turn to the suggestions of Chantler[Chantler, 2000] as implemented in the National Institute of Standards and Technology DTSA-II[1] (a pseudo-acronym) [Ritchie & Newbury, 2012]. Chantler specifies a set of rules based on the X-ray energy and proximity to absorption edges which provide fractional uncertainty estimates. In some regions, the uncertainty estimates exceed 100 %. This is of course problematic as if the uncertainty were distributed in a normal distribution, this would suggest the impossibility of amplification rather than absorption of X-rays. Instead, it seems likely that Chantler was suggesting that the absorption might be much larger than his model suggested under these conditions. Unfortunately, the JCGM:100 Taylor-series approach to uncertainty doesn't handle asymmetric uncertainties. However, the Monte Carlo approach can be used to model arbitrary probability distribution functions (PDFs).

An additional concern is model failure. Equation 24 is an approximation that is known to fail near absorption edges[Newville, 2004]. Large material-to-material deviations in the MACs are most often observed in X-ray microanalysis as a self-absorption problem for X-rays in the L- and M-families. Examples of the effect in EPMA are the Fe L-lines in the Fe-Si system[Gopon et al., 2013] and the Ni L-lines in the Ni-Si system[Llovet et al., 2016]. Slightly below the absorption edge energy, there are pre-edge effects due to local bonding and oxidation state effects. Around the edge energy, the edge may shift as much as 5 eV per unity change in oxidation state. In the region a couple of hundred electron-volts above the absorption energy interatomic distances and bond angles can lead to multiple scattering of the X-rays. Together, these effects are called X-ray absorption near edge structure (XANES) and extended X-ray absorption fine structure (EXAFS) (see Figure 3). It is not clear how to handle these model failures of Equation 24. To an extent, the model fails in the same regions in which the elemental MACs are uncertain and the uncertainty in the elemental MACs will be contribute to the uncertainty in the material MAC. There is however, an additional question of correlation between material MACs computed from the same elemental MACs. Clearly, XANES and EXAFS diminish the correlation between the uncertainty in the energy regions near edges. Materials can have wildly different MACs despite being relatively similar in composition because

[1] DTSA-II is available for free from `https://goo.gl/MI1Ku`

of near edge effects. However, far from edges we don't expect the correlation to be diminished in such a manner.

These considerations are important because it is positive correlation between the material MACs that makes similar standards a useful technique for reducing overall measurement uncertainties in most case. A reasonable way to handle this might be to compute the material MAC and then when the X-ray energy is close to an ionization edge, edit the correlation matrix to reduce the positive correlation between the uncertainties of the materials. This is a little bit *ad hoc* but does seem to have the desired effect. There are a couple of things to remember when editing the correlation matrix. The MAC has contributions from the current edge and lower energy edges too. Thus K edge has contributions from the K shell and from the L- and M-family edges in proportion to the jump-ratio. The jump ratio is the ratio of the MAC immediately above the edge to that immediately below the edge.

Assigning uncertainties to MACs is complex. These observations only touch upon a few of the issues. The subject is worthy of further consideration.

## 2.3 Computing the $k$-ratio

The $k$-ratio is defined as the dose and continuum corrected ratio between the intensity measured on the unknown relative to the intensity measured on the standard[Castaing, 1951]. The $k$-ratio may be computed from data collected on a WDS or EDS although the mechanisms are usually very different. A typical WDS measurement involves measuring 6 intensities at typically 3 different spectrometer positions, two continuum measurements and one on-peak measurement for each of the unknown and the standard. The live-time and probe current associated with each measurement can vary for each measurement. This treatment goes beyond Marinenko and Leigh[Marinenko & Leigh, 2010] in that their treatment assumes that the live-times are equal for the peak and continuum measurements.

Typically, each measured intensity is scaled to counts/(nAs). The scaled continuum intensities are interpolated to estimate the scaled continuum intensity at the on-peak position. The estimated, scaled continuum intensity is subtracted from the scaled on-peak intensity level to give the dose and continuum corrected on-peak characteristic intensity. This process is repeated for both the standard and the unknown.

For $m \in \{u, s\}$, the unknown and standard respectively, and $p \in \{low, high, peak\}$, there are 24 measured values that enter into the $k$-ratio calculation.

$$\begin{array}{ccccc} I_{m,low} & I_{m,high} & I_{m,peak} & \text{Raw intensity measurements} \\ R_{m,low} & R_{m,high} & R_{m,peak} & \text{Spectrometer positions} \\ \tau_{m,low} & \tau_{m,high} & \tau_{m,peak} & \text{Live times} \\ j_{m,low} & j_{m,high} & j_{m,peak} & \text{Probe currents} \end{array} \tag{25}$$

Each of these measured values may have an associated uncertainty.

$$\bar{I}_{m,p} = \frac{I_{m,p}}{j_{m,p}\tau_{m,p}} \tag{26}$$

$$\frac{\partial \bar{I}_{m,p}}{\partial I_{m,p}} = \frac{\bar{I}_{m,p}}{I_{m,p}}$$
$$\frac{\partial \bar{I}_{m,p}}{\partial j_{m,p}} = \frac{-\bar{I}_{m,p}}{j_{m,p}}$$
$$\frac{\partial \bar{I}_{m,p}}{\partial \tau_{m,p}} = \frac{-\bar{I}_{m,p}}{\tau_{m,p}}$$

where $\bar{I}_{m,p}$ is the dose-normalized intensity,

$$\bar{I}_{m,char} = \bar{I}_{m,peak} - \frac{\left(R_{m,peak} - R_{m,low}\right)\bar{I}_{m,high} + \left(R_{m,high} - R_{m,peak}\right)\bar{I}_{m,low}}{R_{m,high} - R_{m,low}} \tag{27}$$

$$\frac{\partial \bar{I}_{m,char}}{\partial \bar{I}_{m,peak}} = 1$$
$$\frac{\partial \bar{I}_{m,char}}{\partial \bar{I}_{m,low}} = \frac{R_{m,peak} - R_{m,high}}{R_{m,high} - R_{m,low}}$$
$$\frac{\partial \bar{I}_{m,char}}{\partial \bar{I}_{m,high}} = \frac{R_{m,low} - R_{m,peak}}{R_{m,high} - R_{m,low}}$$
$$\frac{\partial \bar{I}_{m,char}}{\partial R_{m,peak}} = \frac{\bar{I}_{m,low} - \bar{I}_{m,high}}{R_{m,high} - R_{m,low}}$$
$$\frac{\partial \bar{I}_{m,char}}{\partial R_{m,low}} = \frac{\left(\bar{I}_{m,high} - \bar{I}_{m,low}\right)\left(R_{m,high} - R_{m,peak}\right)}{\left(R_{m,high} - R_{m,low}\right)^2}$$
$$\frac{\partial \bar{I}_{m,char}}{\partial R_{m,high}} = \frac{\left(\bar{I}_{m,low} - \bar{I}_{m,high}\right)\left(R_{m,low} - R_{m,peak}\right)}{\left(R_{m,high} - R_{m,low}\right)^2}$$

where $\bar{I}_{m,char}$ is the characteristic X-ray intensity (continuum corrected),

$$k_{u,s} = \frac{\bar{I}_{u,char}}{\bar{I}_{s,char}} \tag{28}$$

$$\frac{\partial k_{u,s}}{\partial \bar{I}_{u,char}} = \frac{1}{\bar{I}_{u,char}}$$
$$\frac{\partial k_{u,s}}{\partial \bar{I}_{s,char}} = \frac{-\bar{I}_{u,char}}{\bar{I}^2_{s,char}}$$

The 24 measured values represent the input to the calculation. The calculation proceeds by first computing the normalized intensity at each of the 3 positions and 2 materials, $u$ and $s$. In the second step, the normalized intensities from the 3 positions are combined with the 3 spectrometer positions for the 2

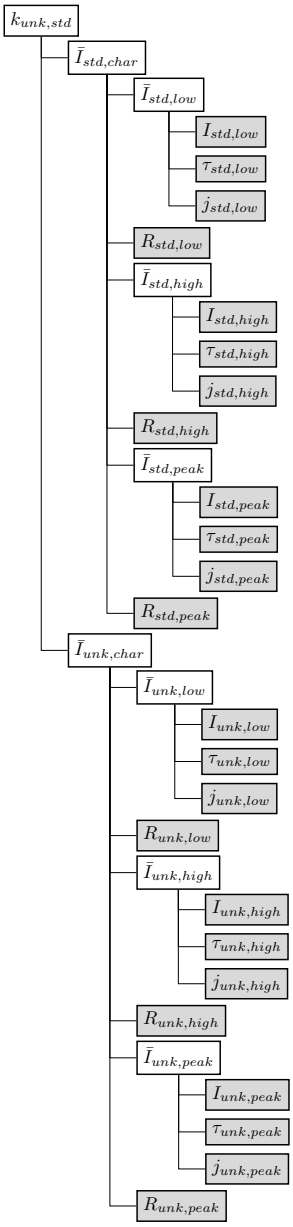


FIGURE 4: *The three level calculation of a k-ratio. Each of the 24 grayed leaf nodes represents an input value potentially with an associated uncertainty. Each non-leaf node represents the result of a calculation.*

materials to calculate the normalized characteristic-only intensity. In the third step, the $k$-ratio is calculated from the 2 normalized intensities. This is shown schematically in Figure 4. The first step represents 6 independent calculations with 3 independent inputs. The second step combines the 3 of the outputs from step one with 3 additional inputs for each material.

It is worth considering how to determine the uncertainties associated with the raw intensities, the spectrometer positions, the live times and the probe currents. The conventional way to handle the raw intensities is to assume that the raw intensities are the result of a Poissonian process[Ancey et al., 1977]. Poissonian processes have well understood PDFs. However, the model can go beyond this to consider such factors as the influence of chemical shifts and other forms of peak shape variation and of variation which results from irreproducibility of the spectrometer position. If *area peak factors*[Bastin & Heijligers, 1986] are used, the uncertainty in the area peak factor can be integrated into the model. The live times can take into account any uncertainties in the dead-time correction protocol. The probe current model can take into account the elapse since the probe current was measured. More recent measurements are likely to be more accurate than less recent measurements. By time stamping our probe current measurements, we can track the stability of our system and build models of each sub-system that reflect the true performance of our instrument. All of these factors can be modeled and these models integrated into the overall measurement model. As the models for each of the input parameters become more sophisticated, our ability to identify the weaknesses in our measurement protocols increase and our abilities to improve the measurement protocols is enhanced.

One of the beauties of this modular/step-wise uncertainty modeling scheme is that adding refinement to the model is relatively easy. For example, we could replace the step in which we compute the normalized intensity with a module that includes area peak factors. An area peak factor involves measuring both the integrated peak intensity and the on-peak intensity. The factor relates the quick-to-measure on-peak intensity to the more representative integrated peak intensity.

There are numerous other schemes for estimating the continuum level under the characteristic peak - like *multi-point continuum models*[Allaz et al., 2019] and *mean-atomic number continuum models*[Donovan et al., 2011; Donovan & Tingle, 1995]. While these methods are more complex, there is fundamentally no reason that similar techniques can not be applied to them to estimate the associated uncertainties. If a multi-point continuum model is shared between multiple characteristic lines, the *shared-background model*[Allaz et al., 2019] introduces a dependency between the elements which will introduce correlations between the $k$-ratios.

## 2.4 The $k$-ratio Protocol

As discussed in Equation 16, the $k$-ratio method of compositional analysis is an implicit measurement model based on a set of coupled equations. As is the case

for implicit models, we are not able to solve explicitly for the desired measured quantities. Instead we use an iterative procedure of successively better approximations to converge on an approximate answer. In matrix correction, this process is typically called "iteration" and there are various algorithms that have historically been used including "simple Newton iteration", "hyperbolic iteration" (or "$\alpha$-factor iteration")[Criss & Birks, 1966], Wegstein iteration[Springer, 1976] and "PAP iteration" [Pouchou & Pichoir, 1991]. While none can be proven to converge in all cases, iteration has been observed to work sufficiently well in the field.

The inputs to the uncertainty calculation for the $k$-ratio method are the set of $k$-ratios, $\mathbf{k}$, the estimated composition of the unknown, $\mathbf{C_u}$, the mass fraction of the $i$-th element in the standard, $C_{s,i}$, and the matrix correction factors relative to the pure element for the unknown and standards, $ZAF_{u,i}$ and $ZAF_{s,i}$. The index $i$ corresponds to the element and transition or set of transitions for which the $k$-ratio is measured and the matrix correction is calculated.

$$h_i = k_i - \frac{C_{u,i}}{C_{s,i}} \frac{ZAF_{u,i}(\mathbf{C}_u)}{ZAF_{s,i}(\mathbf{C}_s)}. \tag{29}$$

It is worthwhile to reflect on the meaning of this equation. The iteration process involves finding the $\mathbf{C}_u$ that make all the $\mathbf{h}$ sufficiently close to zero. Expressed another way, we are trying to find the $k$-ratio computed from the $\mathbf{C}_u$ that equals the measured $k$-ratios, $\mathbf{k}$.

$$\frac{\partial h_i}{\partial k_i} = 1 \tag{30}$$

$$\frac{\partial h_i}{\partial ZAF_{u,j}} = -\frac{C_{u,i}}{C_{s,i}} \tag{31}$$

$$\frac{\partial h_i}{\partial ZAF_{s,j}} = \frac{C_{u,i}}{C_{s,i}} \tag{32}$$

$$\frac{\partial h_i}{\partial C_{u,i}} = -\frac{ZAF_{u,i}(\mathbf{C}_u)}{ZAF_{s,i}(\mathbf{C}_s)} \frac{1}{C_{s,i}} \tag{33}$$

$$\frac{\partial h_i}{\partial C_{s,i}} = \frac{ZAF_{u,i}(\mathbf{C}_u)}{ZAF_{s,i}(\mathbf{C}_s)} \frac{C_{u,i}}{C_{s,i}^2} \tag{34}$$

Applying Equation 14, the Jacobian $\mathbb{J}_\mathbf{y}$ consists of the partial derivatives relative to $C_{u,i}$ and the Jacobian $\mathbb{J}_\mathbf{x}$ consists of the partial derivatives relative to $k_i$, $ZAF_{u,s,j}$, and $C_{s,i}$. The uncertainty matrix $\mathbb{U}_\mathbf{x}$ corresponds to the input uncertainties and we solve the equation for the uncertainty matrix $\mathbb{U}_\mathbf{y}$.

The input uncertainties correspond to the uncertainties in the $k$-ratios, $\mathbf{k}$, the uncertainties in the standards $\mathbf{C}_s$ and the uncertainties in the matrix correction $\mathbf{ZAF}_{u,s}$. Each of these terms must be calculated in a previous sub-calculation. The calculation of $\mathbf{ZAF}_{u,s}$ is sufficiently involved that it will be handled in the second of this series of articles.

This treatment differs from previous treatments [Lifshin et al., 1999; Marinenko & Leigh, 2010] in that it considers the problem as a multivariate measurement model and not simply a series of univariate measurement models. It also considers how uncertainty in the composition of the standard and the other elements in the unknown will influence the uncertainty in the estimated unknown.

While it is necessary to estimate the mass fraction of every element in the unknown, it is not necessary to make all of the estimates from the $k$-ratio measurements. It is also possible to use *unmeasured element* rules like *element-by-difference*, *oxygen-by-stoichiometry* and *waters-of-hydration* to estimate hard to measure elements. Implementation of these rules are described in Sections 2.1.3 and 2.1.4. These rules should be applied the step following the implicit $k$-ratio model step.

# 3 Building the model calculation

As was the case in Section 2.3, a complex calculation is often formed by combining many simpler calculations. In practice, two ways in which sub-calculations may be combined could be described as *in-parallel* and *in-series*. In the in-parallel mode, independent sub-calculations can be combined into a single step represented by a larger Jacobian. An example of this are the 6 dose corrected intensities calculated as in Equation 26. While the sub-calculations may use the same set of input parameters, the output of one sub-calculation can not be the input to another. In in-series mode, the calculation is broken into steps in which the output of one step becomes the input to a subsequent step. For example, the 6 dose corrected intensities in Equation 26 must be calculated before being used in Equation 27. The $k$-ratio calculation can be easily implemented in three in-series steps by computing the dose corrected intensities in step 1, the dose and continuum corrected intensities in step 2, and the $k$-ratio in step 3.

In a multi-step serial calculation, it is common that the input (not just the output) from one step will be required as an input to a subsequent step. It is thus useful to be able to carry input values from one step to the next step. This is trivially implemented by adding a row to the Jacobian associated with the function $f_j(\mathbf{X}) = X_i$ where $X_i$ is the input parameter.

It is critical that each parameter in the model is represented by one-and-only-one parameter in the input uncertainty matrix. If the same value is used in different places in the same calculation, they must all refer back to the same elements in the uncertainty matrix. Vice versa, two values might seem to be equivalent but actually share different provenances with different uncertainty characteristics and should be represented by different entries in the uncertainty matrix. An example is analyzing natural uranium using a depleted uranium standard. The mean atomic weights of natural and depleted uranium are different and have different uncertainties. It sometimes requires subtle insight to determine whether a parameter should be shared. An example of this subtlety is computing material MACs from elemental MACs, a topic which is sufficiently

important and complex as to deserve a paper of its own. Another example is the mass-thickness of a coating used to make a insulating sample conductive. If samples were coated simultaneously it is reasonable to expect the mass-thickness of the samples coatings to be highly correlated (and consistent). Simultaneously coated samples should be represented by a single mass-thickness value. However, if samples were coated at different times, the mass-thickness might be better represented by a separated value (with independent uncertainties) for each sample.

Implementing all this becomes an issue of bookkeeping - keeping track of which rows and columns contain which output and input values. This can be a particular challenge in microanalysis in which the number of inputs and output varies with the problem and measurement protocol and can easily reach over one-hundred. It helps to have software that facilitates labeling quantities and tracking these quantities through the uncertainty and Jacobian matrices. It helps to have software that permits combining sub-calculations in both serial and parallel modes. It helps to have software that analyzes the full calculation to determine which parameters are calculated and which parameters must be passed as input. It also helps if the software can carry inputs from one step to the next and determine when a parameter is no longer required either as an input to a subsequent step or as final output and then drop it from the calculation. We have implemented such software to facilitate these calculations as a library called *JUncertainty*. This library implements the ideas in JCGM:101 and JCGM:102 in Oracle's Java programming language[2] (`https://www.java.com/`) using the numerical algorithms from the Apache Commons Math library (`https://commons.apache.org/proper/commons-math/`). The source is available for both implementations of the Java language and Apache library. The source code we have developed is available at `https://github.com/usnistgov/Roentgen`.

## 3.1 Interpretation

Working with and interpreting covariance matrices is more challenging than the single variable approach with which we are familiar. Throughout the calculation, it is important to maintain the covariance matrix representation to ensure that the uncertainty relationships between variables are maintained. Typically, sources of uncertainty enter into most calculations as single variables with an associated uncertainty. For example, a measure of intensity with an uncertainty equal to the square-root of the number of counts or a probe current measure with an estimate of the associated uncertainty. However, this need not be the case. For example, in the Committee On Data (CODATA) "Internationally Recommended 2018 Values of the Fundamental Physical Constants"[Tiesinga et al., 2019], the defined constants are without error and measured constants are expressed with the best estimate of the uncertainty. The CODATA web page provides a mechanism to extract the covariance between two measured physical constants.

[2]Disclaimer: Any mention of commercial products is for information purposes only; it does not imply recommendation or endorsement by NIST.

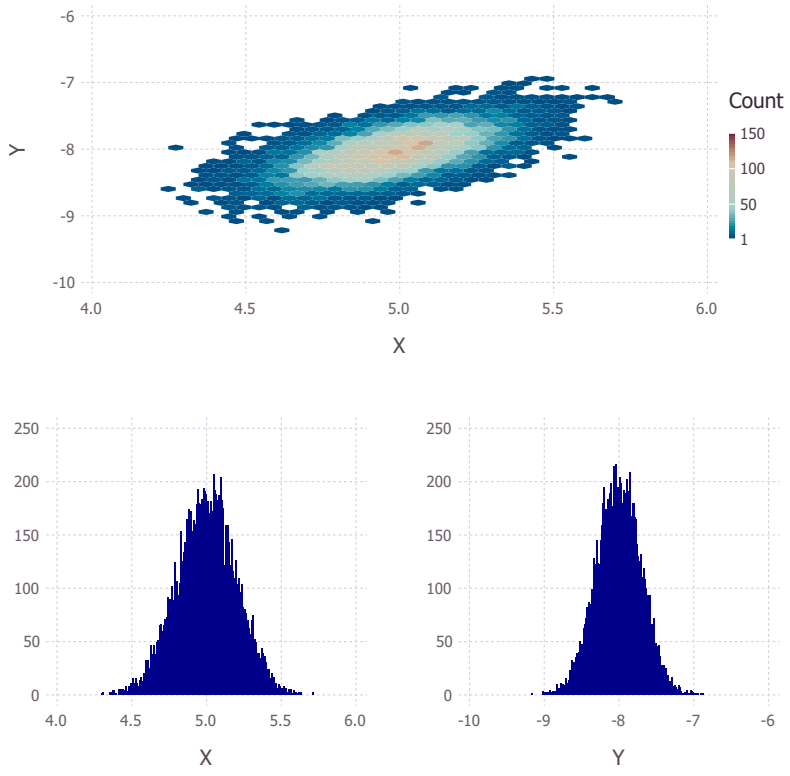


FIGURE 5: *An example of ten-thousand measurements drawn from two correlated random variables drawn from a normal distribution with* $X = 5.0 \pm 0.2$ *and* $Y = -8.0 \pm 0.3$ *with a correlation coefficient of 0.6. The top plot shows the relationship between the two variables and the bottom plots show each variable considered independently.*

When we ask what uncertainty we expect to see for the measurement of a particular value, we are essentially projecting the covariance matrix onto a measuring device which extracts the particular variance associated with the specific variable. Consider for example, Figure 5 which shows the hypothetical situation consisting of two normally distributed random variables of Type A with values $X = 5.0 \pm 0.2$ and $Y = -8.0 \pm 0.3$ related with a correlation coefficient of 0.6. If we measured the variable $X$ ten-thousand times we would expect to see a histogram like that shown in the lower-left of Figure 5. This histogram has a mean of approximately 0.5 and $\sigma_X = 0.2$. Likewise, if we measured the variable $Y$ ten-thousand times we'd expect to see a histogram like that shown in the lower-right. This histogram has a mean of approximately $-8.0$ and $\sigma_Y = 0.3$ So the values $\sigma_X = 0.2$ and $\sigma_Y = 0.3$ are the appropriate values to report as uncertainties associated with $X$ and $Y$. However, if the values $X$ and $Y$ are to be used in subsequent calculations, it is important to retain the full covariance matrix to ensure that the uncertainties associated with the results of the subsequent calculations account for the correlation between $X$ and $Y$.

# 4 Conclusion

JCGM:100 defines two types of sources of uncertainty - Type A and Type B. Type A being those sources whose magnitude can be evaluated by "a statistical analysis of a series of measurements" and Type B being those whose magnitude is determined by other means. While we have focused on the uncertainty associated with the input parameters, both Type A and Type B, there is also an uncertainty associated with the model. For example, in $\phi(\rho z)$-style matrix correction, the shape of the $\phi(\rho z)$ curve is chosen to be an analytical expression that is similar to the distribution observed in tracer measurements or in Monte Carlo simulations[Pouchou & Pichoir, 1991]. A mathematical model that is assumed to describe a process without proven justification is sometime called an *ansatz*. The ansatz can then be parameterized in terms of other pieces of information we can calculate from the physical distribution like the integral of the area under the curve. Model uncertainty due to an ansatz can be viewed as a separate source of uncertainty which is not handled readily by the JCGM:100 framework. One possible way to handle this other source of uncertainty is to consider many different ansatz. Fortunately in matrix correction, there is a proliferation of different models of vary effectiveness. This was the approach taken by the program TRYZAF[Armstrong et al., 2013]. This mechanism should be viewed as complementary to the approach presented in this paper.

One of the biggest sticking points when one approaches uncertainty analysis is determining suitable uncertainties for the Type B input parameters. This can be overwhelming. There are no "correct" answers. The literature is rife with values without uncertainties. Often the best we can do is use our professional judgement to make an educated guess. It is easy to argue that these guesses are wrong - too optimistic or too pessimistic. One analysts judgement about the state of a certain parameter may be very different from another analysts and

we should be having these conversations. However, we can all agree that zero is not the correct answer and that waiting until we have the "perfect" answer doesn't help us to understand the measurement process.

This first article presents a new strategy for calculating uncertainties in X-ray microanalysis measurements. This strategy was applied to some simple modules within the larger problem of matrix corrected measurements of composition. While the strategy initially looks complex, it has a couple of significant advantages which make it easier to apply to complex multi-step measurement models. Through application of the chain-rule of differential calculus, it is possible to divide complex problems into a series of simpler steps. The steps can be made simple enough that the required partial derivatives can be easily evaluated. After evaluation, each step becomes a matrix which can be manipulated using readily available matrix algebra routines. Steps can be mixed-and-matched to produce a flexible model that can be adjusted to fit the measurement model. This is particularly valuable for X-ray microanalysis in which the number of elements and the character of the standards can vary. Furthermore, the input uncertainties can be tracked through to their contributions to the output uncertainties. This allows us to model the sensitivity of the output values to the input uncertainties and facilitates measurement optimization.

In this article, a handful of simpler but necessary steps were identified and the strategy applied. In the next article, the strategy will be applied to a significantly more complex problem - matrix correction. Matrix correction is a model involving tens if not hundreds of input parameters each of which can have an associated uncertainty. Depending upon the measurement conditions, choice of standard and other measurement model choices, different parameters can dominate the final uncertainty.

In the next article, JCGM:102 will be applied to the simplified matrix correction model of Pouchou and Pichoir (also known as *XPP*)[Pouchou & Pichoir, 1991]. This model requires a multivariate measurement model to handle the inter-dependencies between the matrix corrections for each of the measured elements. The model is dynamic in the sense that the number of input variables and output variables depends upon the choice of standards and unknowns. It might be possible to compute the derivative of the output variables with respect to the input variables directly using symbolic mathematics software. However, the resulting expression would be exceeding lengthy and would need to be recalculated each time the unknown or a standard changed. The Jacobian-based model makes it possible to compose multiple computational steps based on the particulars of the standards and the unknown using the multivariate chain rule. The steps can be composed to readily handle changes in the standards or unknown. While the overall calculation remains complex, each individual step can be sufficiently simple to be easily evaluated and efficiently computed. The second article will also contain several examples which show the dependence of the accuracy of the matrix correction model on the instrumental parameters and standard choice.

# References


Allaz, J.M., Williams, M.L., Jercinovic, M.J., Goemann, K. & Donovan, J. (2019). Multipoint background analysis: Gaining precision and accuracy in microprobe trace element analysis, *Microscopy and Microanalysis* **25**, 3046.

Ancey, M., Bastenaire, F. & Tixier, R. (1977). Statistical control and optimization of x-ray intensity measurements, *Journal of Physics D-applied Physics* **10**, 817–830.

Armstrong, J.T. (2014). Comparative performance of SDD-EDS and WDS detectors for quantitative analysis of mineral specimens: The next generation electron microprobe, *Microscopy and Microanalysis* **20**, 692–693.

Armstrong, J.T., Donovan, J. & Carpenter, P. (2013). CALCZAF, TRYZAF and CITZAF: the use of multi-correction-algorithm programs for estimating uncertainties and improving quantitative x-ray analysis of difficult specimens, *Microscopy and Microanalysis* **19**, 812–813.

Bastin, G.F. & Heijligers, H.J.M. (1986). Quantitative electron probe microanalysis of carbon in binary carbides. Iprinciples and procedures, *X-ray Spectrometry* **15**, 135–141.

Bullock, E.S. (2019). A Combined WDS, EDS and Cathodoluminescence Study of Carbonate Grains in Water-Rich Meteorites, *Microscopy and Microanalysis* **25**, 266267.

Camus, P. (2015). Factors Affecting WDS Performance Superiority over EDS, *Microscopy and Microanalysis* **21**, 16291630.

Castaing, R. (1951). *Application des sondes électronique à une méthode d'analyse ponctuelle chimique et cristallographique*, Ph.D. thesis, University of Paris, publication ONERA No. 55 (1952).

Chantler, C.T. (2000). Detailed tabulation of atomic form factors, photoelectric absorption and scattering cross section, and mass attenuation coefficients in the vicinity of absorption edges in the soft x-ray (z= 30-36, z= 60-89, e= 0.1 kev-10 kev), addressing convergence issues of earlier work., *J Phys Chem Ref Data* **29**, 597–1048.

Criss, J. & Birks, L. (1966). 217, Wiley: New York.

Donovan, J.J., Lowers, H.A. & Rusk, B.G. (2011). Improved electron probe microanalysis of trace elements in quartz, *American Mineralogist* **96**, 274–282.

Donovan, J.J. & Tingle, T.N. (1995). An Improved Mean Atomic Number Background Correction for Quantitative Microanalysis, Etz, ES (ed.), *Microbeam Analysis 1995 - Proceedings of the 29th Annual Conference of the*

*Microbeam Analysis Society*, MICROBEAM ANALYSIS, 209–210, 29th Annual Conference of the Microbeam-Analysis-Society, BRECKENRIDGE, CO, AUG 06-11, 1995.

Gopon, P., Fournelle, J., Sobol, P.E. & Llovet, X. (2013). Low-voltage electron-probe microanalysis of Fe-Si compounds using soft x-rays, *Microscopy and Microanalysis* **19**, 16981708.

Heinrich, K.F. (1981). *Electron Beam X-ray Microanalysis*, Van Nostrand Reingold, New York.

JCGM (Joint Committee for Guides in Metrology) (2008). Evaluation of Measurement Data-Guide for the Expression of Uncertainty in measurement. JCGM 100: 2008, *International Organization for Standardization, Geneva* 167.

JCGM (Joint Committee for Guides in Metrology) (2008). Supplement 1 to the Guide to the Expression of Uncertainty in Measurement - Propagation of Distributions Using a Monte Carlo Method." (BIPM 101: 2008), *International Organization for Standardization, Geneva* .

JCGM (Joint Committee for Guides in Metrology) (2011). Evaluation of Measurement Data – Supplement 2 to the "Guide to the Expression of Uncertainty in Measurement - Extension to Any Number of Output Quantities (BIPM:102), *International Organization for Standardization (ISO)* .

Lifshin, E., Doganaksoy, N., Sirois, J. & Gauvin, R. (1999). Statistical considerations in microanalysis by energy-dispersive spectrometry, *Microscopy and Microanalysis* **4**, 598–604.

Llovet, X., Pinard, P.T., Heikinheimo, E., Louhenkilpi, S. & Richter, S. (2016). Electron Probe Microanalysis of Ni Silicides Using Ni-L X-Ray Lines, *Microscopy and Microanalysis* **22**, 12331243.

Marinenko, R.B. & Leigh, S. (2010). Uncertainties in electron probe microanalysis, *IOP Conference Series: Materials Science and Engineering*, vol. 7, 012017, IOP Publishing.

McNaught, A.D. & Wilkinson, A. (eds.) (1997 (downloaded 24-Mar-2020)). *IUPAC Compendium of Chemical Terminology. (The "Gold Book")*, Oxford, UK: Blackwell Scientific Publications, 2nd ed., URL `https://doi.org/10.1351/goldbook`.

Moran, K. & Wuhrer, R. (2016). Current State of Combined EDS-WDS Quantitative X-Ray Mapping, *Microscopy and Microanalysis* **22**, 9293.

Newbury, D.E. & Ritchie, N.W.M. (2015). Quantitative Electron-Excited X-Ray Microanalysis of Borides, Carbides, Nitrides, Oxides, and Fluorides with Scanning Electron Microscopy/Silicon Drift Detector Energy-Dispersive

Spectrometry (SEM/SDD-EDS) and NIST DTSA-II, *Microscopy and Microanalysis* **21**, 1327–1340, 11th Region Workshop of the European-Microbeam-Analysis-Society (EMAS), Leoben, AUSTRIA, SEP 21-24, 2014.

Newbury, D.E. & Ritchie, N.W.M. (2016a). Electron-Excited X-Ray Microanalysis at Low Beam Energy: Almost Always an Adventure!, *Microscopy and Microanalysis* **22**, 735–753.

Newbury, D.E. & Ritchie, N.W.M. (2016b). Measurement of Trace Constituents by Electron-Excited X-Ray Microanalysis with Energy-Dispersive Spectrometry, *Microscopy and Microanalysis* **22**, 520–535.

Newbury, D.E. & Ritchie, N.W.M. (2018). An iterative qualitativequantitative sequential analysis strategy for electron-excited x-ray microanalysis with energy dispersive spectrometry: Finding the unexpected needles in the peak overlap haystack, *Microscopy and Microanalysis* **24**, 350373.

Newville, M. (2004). Fundamentals of XAFS, *Consortium for Advanced Radiation Sources, University of Chicago (USA)[http://xafs org]* **78**.

Pouchou, J.L. & Pichoir, F. (1991). Quantitative analysis of homogeneous or stratified microvolumes applying the model 'PAP', K. Heinrich & D. Newbury (eds.), *Electron Probe Quantitation*, 31–75, Springer, URL `http://www.ebook.de/de/product/3835664/electron_probe_quantitation.html`.

Reed, S. & Mason, P. (1967). *Transactions of the Second National Conference on Electron Microprobe Analysis* .

Ritchie, N.W.M. & Newbury, D.E. (2012). Uncertainty Estimates for Electron Probe X-ray Microanalysis Measurements, *Analytical Chemistry* **84**, 9956–9962.

Springer, G. (1976). Iterative procedures in electron probe analysis corrections, *X-Ray Spectrometry* **5**, 88–91.

Terborg, R. & Richter, S. (2019). Analysis and Quantification of Transition Metal Borides with WDS and EDS, *Microscopy and Microanalysis* **25**, 17661767.

Thompson, K. (2018). Advances in SDD-based EDS and Comparisons to WDS for Light Element Sensitivity, *Microscopy and Microanalysis* **24**, 754755.

Tiesinga, E., Mohr, P.J., Newell, D.B. & Taylor, B.N. (2019). The 2018 CODATA Recommended Values of the Fundamental Physical Constants" (Web Version 8.0), Website Version 8.0, National Institute of Standards and Technology, Gaithersburg, MD, URL `http://physics.nist.gov/constants`, Database developed by J. Baker, M. Douma, and S. Kotochigova.

Ziebold, T.O. (1967). Precision and sensitivity in electron microprobe analysis, *Analytical Chemistry* **39**, 858–861.